Supplementary Information (SI) for Soft Matter.

Supplementary Materials

Effect of Droplet Deposition on Aerosol Capture Efficiency of Bipolarly Charged Fibers

A. Kumar,[1] S. Gautam,[1] N. Bhatta,[1] H.V. Tafreshi,[1,2,*] and B. Pourdeyhimi [2]
[1]*Department of Mechanical and Aerospace Engineering, NC State University, Raleigh, NC 27695-7910, United States*
[2]*The Nonwovens Institute, NC State University, Raleigh, NC 27606, United States*

S1. Numerical procedure

Our numerical simulations were conducted using ANSYS CFD code enhanced with a series of in-house user defined functions (UDFs) developed to solve the electrohydrodynamic field and to perform particle tracking, as detailed in Sections 2 and 3. For pressure-velocity coupling, the SIMPLE algorithm was used along with the Modified Body Force Weighted scheme for pressure discretization. The air–liquid interface (ALI) reconstruction was performed by considering the Geo-reconstruct scheme. For the electrostatic domain, we defined two user-defined scalar equations: one for electrostatic potential and the other for the electrostatic charge. Each term of the charge conservation equation was specified using a UDF. In addition, the first and second term of Eq. 5 were added to the electrohydrodynamic module in ANSYS via another UDF. After the droplets reached an equilibrium shape on the fiber surface, the coordinates of each deposited droplet were saved to be used for marking the cells that collectively represented the shape of the droplets. Twelve user-defined memories (UDMs), denoted as UDM0 through UDM11, were developed and used in ANSYS environment. These UDMs were accessed via an in-house UDF program. Initially set to zero, all UDMs were assigned to every computational cell in the domain. Upon occupancy by a deposited droplet,

*Address correspondence to Hooman V. Tafreshi, email: hvtafres@ncsu.edu; tel.: 919-515-6151;
URL: http://mae.ncsu.edu/pmmf/

the UDM0 value of the respective cells was updated to unity. Likewise, when a cell became occupied by an ALI, its UDM1 was set to unity. UDM2 to UDM10 were employed to store the volumetric charge density, as well as the magnitude, components, and the gradient of the electrostatic field across the entire computational domain. Moreover, once the cells occupied by deposited droplets were marked, a non-zero permeability constant of $K_p = 1 \times 10^{-8} m^2$ was assigned to them using UDM11. This was done to avoid numerical divergence. Subsequently, numerical simulations of aerosol filtration by a droplet-loaded electret fiber were conducted by solving the governing equations described in Section 3. An adjusted UDF code was integrated into ANSYS to calculate the electrostatic forces (polarization and Coulomb) exerted on the airborne particles. These forces were calculated using the magnitude, components, and gradient of the electrostatic field stored in UDMs during the electrohydrodynamic simulation, along with the diameter and charge-to-mass ratio of the injected aerosol particles. Each particle size group underwent two simulations, one with positive particles and the other with negative particles, and the results were subsequently averaged and presented in the results and discussion Section. A flowchart for our numerical procedure is given in Figure S1.

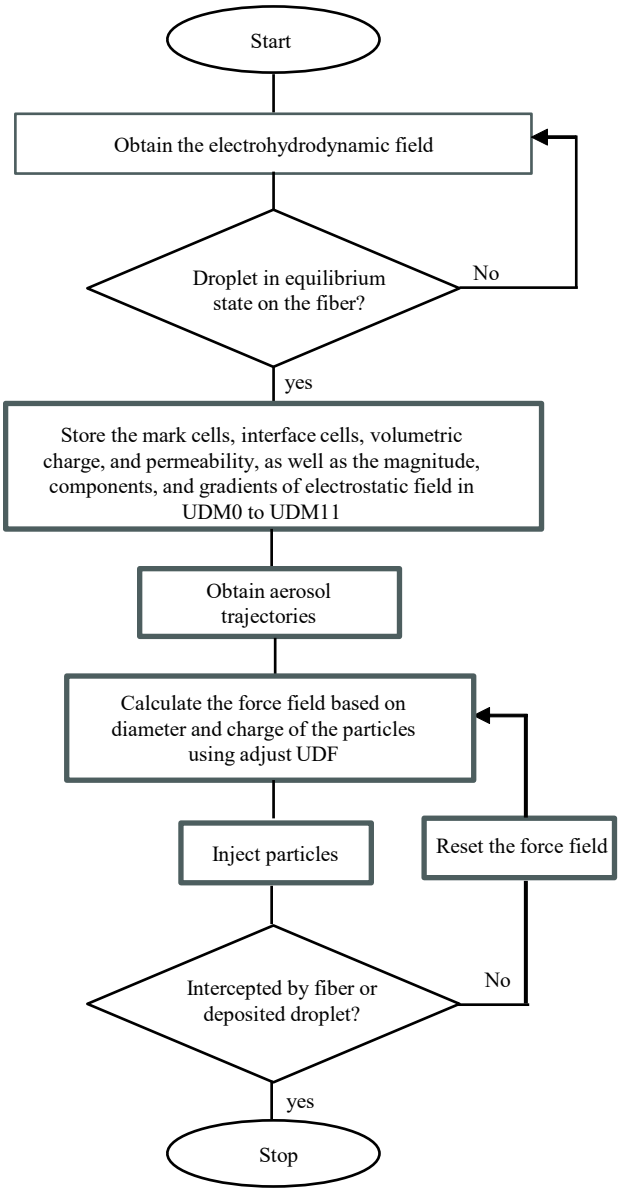

Figure S1: Flowchart for particle tracking process.

S2. Empirical Equations for Single Fiber Efficiency

The SFE of an electret filter due to Coulomb force can be estimated using Eq. (A1) [1, 2].

$$E_{\sigma C}(n) = \left(\frac{1-\alpha}{Ku}\right)^{\frac{1}{8}} \frac{\pi N_{CD}(n)}{1 + 2\pi[N_{CD}(n)]^{\frac{1}{4}}} \quad \text{(A1)}$$

Here, α represents the solid volume fraction of the filter, Ku denotes the Kuwabara factor, and $N_{CD}(n)$ is the ratio of the Coulomb force to the inertial force.

$$Ku = -\frac{ln\alpha}{2} - 0.75 + \alpha - 0.25\alpha \quad \text{(A2)}$$

$$N_{CD}(n) = \frac{C^c \sigma_f q(n)}{3\pi\mu\varepsilon_0(1+\varepsilon_f)d_f U_0} \quad \text{(A3)}$$

where, σ_f, ε_f, d_f and U_0 represent the surface charge density, relative permittivity, fiber diameter, and face velocity, respectively. Similarly, the SFE due to the polarization force is obtained using Eq. (A4)

$$E_{\sigma D} = \left(\frac{1-\alpha}{Ku}\right)^{\frac{2}{5}} \frac{\pi N_{DD}}{1 + 2\pi N_{DD}^{\frac{2}{3}}} \quad \text{(A4)}$$

Here, N_{DD} stands for the ratio of the electrostatic force (attributed to polarization) to the inertial force.

$$N_{DD} = \frac{2\, C^c \sigma^2 {d_p}^2}{3\mu\varepsilon_0(1+\varepsilon_f)^2 d_f U_0}\left(\frac{\varepsilon_p - 1}{\varepsilon_p + 2}\right) \quad \text{(A5)}$$

The collection efficiency of a filter depends greatly on the charge distribution of the particles. In our study, we assumed the size of airborne particles ranging from 50 to 1000 nm and carried a single positive or negative charge (i.e., $q_p = \pm 1e$) with an equal number distribution.

The SFE due to interception relies on the ratio of the particle diameter to the fiber diameter, and given as,

$$E_r = \frac{(1-\alpha)r^2}{Ku(1+r)} \quad \text{(A6)}$$

where *r* is given as,

$$r = \frac{d_p}{d_f} \tag{A7}$$

Therefore, in this study, the total single fiber efficiency (SFE) was determined by combining the individual efficiencies of the polarization, Coulombic, and interception mechanisms, as given in Eq. (A8)

$$\eta_{SFE}(n) = 1 - \left(1 - E_{\sigma D}(n)\right)\left(1 - E_{\sigma C}(n)\right)\left(1 - E_r(n)\right) \tag{A8}$$

Furthermore, it was assumed that particles carried a single positive or a single negative charge (i.e., $q_p = \pm 1e$) with an equal number distribution. Therefore, two simulations were conducted for each particle size group, one with the positive particles and the other with the negative particles, and the results were averaged as shown in Eq. (A9)

$$\eta_{SFE} = \frac{\eta_{SFE}(n = -1) + \eta_{SFE}(n = +1)}{2} \tag{A9}$$

S3. Validation of Electrohydrodynamic Flow Modeling

To validate our VOF simulation of droplet deposition on the fiber in the presence of an electrostatic field, we compared the results of our simulations with experimental data reported under identical operating conditions by Torza et al. [3] (considered in many studies as an accurate experiment suitable for model validation). In their research, these authors used silicone oil as the droplets and oxidized castor oil as the surrounding fluid. Due to the conductive nature of the fluids used in the experiment, we considered a leaky dielectric model for our simulations. Based on the fluid properties provided in Torza et al., [3] (class C, system 16), we conducted transient simulations in a 4 cm by 1.7 cm rectangular domain. We considered a droplet diameter of d = 0.0734 cm. These simulations spanned different values of the electrical capillary number Ca_E, defined as the ratio of electrical force to surface tension force. After reaching a a stable drop shape, we determined the drop deformation factor D using Eq. A11.

$$D = \frac{L - B}{L + B} \tag{A11}$$

Here, L represents the end-to-end length of the droplet measured along the electric field, while B denotes the maximum end-to-end width in the perpendicular direction to the electric field. Positive and negative deformations of the droplet signify the steady state prolate and oblate shapes, respectively. Figure S2 compares the droplet's deformed shapes from experiments (a-c) and from our simulations (d-f). This comparison reveals a close agreement between the deformation factors predicted by the numerical simulation and measured experimentally. Additionally, our numerical results were compared with data from Taylor's empirical equation, Eq. A12 [4].

$$D = \frac{9 f_d(R,Q,\lambda)}{8(2 + R)^2} Ca_E \tag{A12}$$

$$f_d(R,Q,\lambda) = R^2 + 1 - 2Q + \frac{3}{5}(R - Q)\frac{(2 + 3\lambda)}{(1 + \lambda)} \tag{A13}$$

$$Ca_E = \frac{\left(E^2 \varepsilon_0 d\right)}{2\gamma} \tag{A14}$$

The percentage differences between our numerical results and both the experimental data and the predictions from Taylor's empirical equation were less than 1.4% and 2.4%, respectively, for the lowest electrical capillary number, and 4.26% and 25.0%, for the highest. The larger discrepancy between our numerical results and the predictions from Taylor's equation is because Taylor's empirical equation was developed with the assumption of small droplet deformations (i.e., for low electrical capillary numbers).

Droplet deformation factor prediction	Electrical capillary number (Ca_E)		
	0.137	0.380	0.745

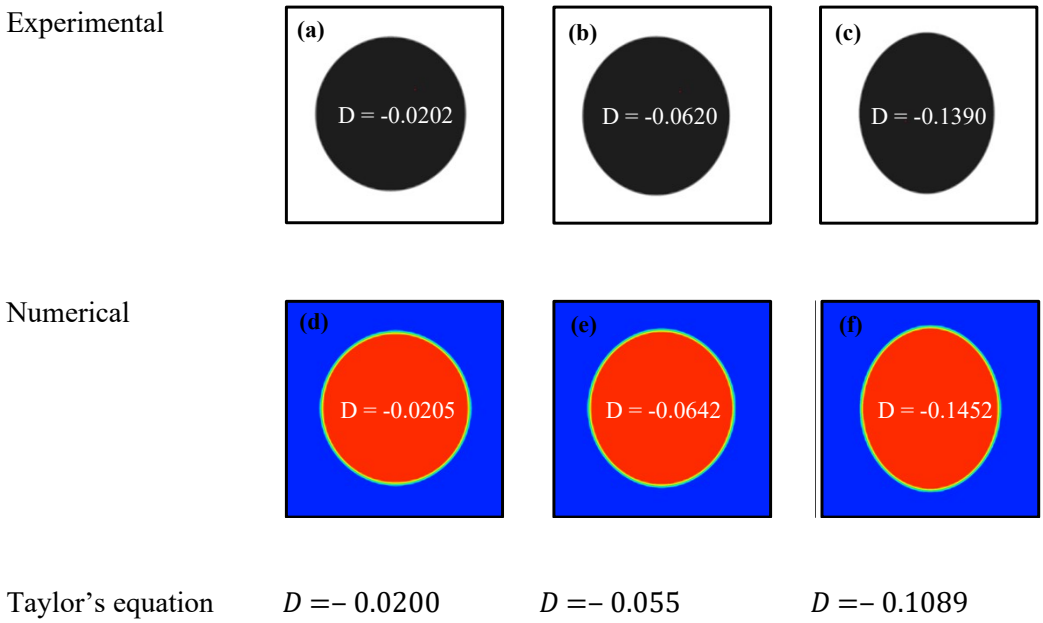

Figure S2: Depicts a comparison of droplet deformation observed in the experiments of Torza et al. (a-c) in the first row, predicted in numerical simulations using the leaky dielectric model (d-f) the second row and calculated using Taylor's empirical equation in the third row. Where *D* is deformation factor. The test conditions are as follows: R <0.033, Q =0.44 and Ca_E is changed from left to right at 0.136, 0.380 and 0.745, respectively.

S3. Validation of Aerosol Flow Modeling

We also compared our numerical simulation of particle filtration with the predictions of empirical correlations from Section 2 of Supplementary Material. For further details on the validation of the aerosol flow model, interested readers can refer to our previous work [5].

REFERENCES

[1] R.C. Brown, D. Wake, R. Gray, D. B. Blackford and G. J. Bostock, Effect of industrial aerosols on the performance of electrically charged filter material, Annals of Occupational Hygiene, 1988, 32, 271-294.

[2] R. H.J.S. Lathrache, H. J. Fissan, S. Neumann, Deposition of submicron particles on electrically charged fibers. Journal of Aerosol Science, 1986, 17 (3), 446−449.

[3] S. Torza, R. G. Cox, S. G. Mason, Electrohydrodynamic deformation and burst of liquid drops, Philosophical Transactions Royal Society London, 1971, 269, 295-319.

[4] G. Taylor, Studies in electrohydrodynamics, I: The circulation produced in a drop by electrical field, Proc. R. Soc. London, 1966, 291, 159.

[5] A. Kumar, S. Gautam, S. Atri, H.V. Tafreshi, B. Pourdeyhimi, Importance of Dipole Orientation in Electrostatic Aerosol Filtration, Langmuir, 2023, 39, 17653-17663.